

# Discoveries of 3 K-shell Lines of Iron and a Coherent Pulsation of 593-sec from SAX J1748.2–2808

Masayoshi NOBUKAWA, Katsuji KOYAMA, Hironori MATSUMOTO, and Takeshi Go TSURU  
*Department of Physics, Graduate school of Science, Kyoto University, Sakyo-ku, Kyoto 606-8502*  
*nobukawa@cr.scphys.kyoto-u.ac.jp, koyama@cr.scphys.kyoto-u.ac.jp*

(Received 2008 May 19; accepted 2008 June 22)

## Abstract

SAX J1748.2–2808 is a unique X-ray object with a flat spectrum and strong emission lines at 6.4–7.0 keV. The Suzaku satellite resolved the emission lines into 3 K-shell lines from neutral and highly ionized irons. A clear coherent pulsation with a period of 593-sec was found from the Suzaku and XMM-Newton archives. These facts favor that SAX J1748.2–2808 is an intermediate polar, a subclass of magnetized white dwarf binary (cataclysmic variable: CV). This paper reports on details of the findings and discusses the origin of this source.

**Key words:** Galaxy: Center—Magnetic Cataclysmic Variable —Intermediate Polar — X-ray spectra

## 1. Introduction

SAX J1748.2–2808 was discovered with the Beppo-SAX satellite in the direction of the radio complex Sagittarius (Sgr) D (Sidoli et al. 2001), and was deeply re-observed with the XMM-Newton satellite (Sidoli et al. 2006). The X-ray spectrum was well-fitted with a power-law of photon index 1.4 plus a broad line of 0.43 keV ( $1\sigma$ ) with the center energy at 6.6 keV. The  $N_{\text{H}}$  value was as large as  $1.4 \times 10^{23}$  H cm $^{-2}$  (Sidoli et al. 2006). SAX J1748.2–2808 was thus regarded as one of the brightest samples of resolved point sources in the Galactic center region (GC) with Chandra deep-exposure observations (Muno et al. 2003, Muno et al. 2006). The integrated spectra of the point sources resemble the Galactic center diffuse X-rays (GCDX) in the iron line features close to 6.4–7.0 keV (Muno et al. 2004, Koyama et al. 2007b). Therefore, these, including SAX J1748.2–2808, can be regarded as significantly contributing to the GCDX, even though SAX J1748.2–2808 was brighter than most of the other point sources in the GC.

The XMM-Newton spectrum favored that SAX J1748.2–2808 is a High Mass X-ray Binary (HMXB) pulsar located at the GC region (Sidoli et al. 2006). However, no coherent pulsation was reported from either the Beppo-SAX or the XMM-Newton observations. Furthermore, the broad line of 0.43 keV ( $1\sigma$ ) is very unusual as a HMXB. If this broadening is due to the Doppler effect, the velocity dispersion is as large as  $2 \times 10^4$  km s $^{-1}$ . No such HMXB has been reported so far (e.g. Nagase 1989). The detailed spectrum of SAX J1748.2–2808 did not indicate whether the spectral nature is thermal or non-thermal.

In order to understand the nature of this unique object, we analyzed the Suzaku data of two pointing observations on the supernova remnants (SNR), Sgr D SNR and G 0.9+0.1, and also re-analyzed the XMM-Newton archive data.

## 2. Observations and Data Reduction

The Suzaku and XMM-Newton observations of SAX J1748.2–2808 are listed in table 1. The Suzaku satellite observed the two SNRs, Sgr D SNR and G 0.9+0.1, where SAX J1748.2–2808 was located near the edge of the field of view (FOV) of the XIS. The XIS consists of four sets of X-ray CCD camera systems (XIS 0, 1, 2, and 3) placed on the focal planes of four X-Ray Telescopes (XRT) aboard the Suzaku satellite. XIS 0, 2, and 3 have front-illuminated (FI) CCDs, while XIS 1 has a back-illuminated (BI) CCD. One of the FI CCD cameras (XIS 2) has been out of function since September, 2006, and hence we did not use it. Detailed descriptions of the Suzaku satellite, the XRT, and the XIS can be found in Mitsuda et al. (2007), Serlemitsos et al. (2007), and Koyama et al. (2007a).

The XIS observations were made with the normal mode. The XIS pulse-height data for each X-ray event were converted to Pulse Invariant (PI) channels using the `xispi` software version 2007-03, and the calibration database version 2008-01-31. We removed the data during the epoch of low-Earth elevation angles less than 5 degrees ( $\text{ELV} < 5^\circ$ ), day Earth elevation angles less than 10 degrees ( $\text{DYE\_ELV} < 10^\circ$ ), and the South Atlantic Anomaly. The good exposure times are listed in table 1. Although the XIS CCDs were significantly degraded by on-orbit particle radiation, the CCD performances were restored by the Spaced-low charge injection technique (Uchiyama et al. 2009). Then, the overall spectral resolutions at 5.9 keV were  $\sim 150$  and  $\sim 170$  eV (FWHM) for the FI and BI CCDs, respectively. We analyzed the data using the software package HEASoft 6.4.1. For the spectral fittings, we made XIS response files using `xisrmfgen`, and auxiliary files using `xissimarfgen`. Since the spectrum of the non-X-ray background (NXB) depends on the geomagnetic cut-off rigidity (COR) (Tawa et al. 2008), we obtained COR-sorted NXB spectra using `xisnxbgen`, from

**Table 1.** Observation data list

Observatory/Instrument	Target	Obs. ID	Date (yyyy/mm/dd)	Good Exposure Time* (ksec)
Suzaku/XIS	Sgr D SNR	502020010	2007/09/06	139.1
Suzaku/XIS	G 0.9+0.1	502051010	2008/03/11	138.8
XMM-Newton/MOS	Sgr D SNR	0112970101	2000/09/23	15.7
XMM-Newton/PN	Sgr D SNR	0112970101	2000/09/23	11.5
XMM-Newton/MOS	G 0.9+0.1	0144220101	2003/03/12	49.5
XMM-Newton/MOS	SAX J1748.2–2808	0205240101	2005/02/26	50.2
XMM-Newton/PN	SAX J1748.2–2808	0205240101	2005/02/26	41.5

\* After the data screening described in the text.

the night-Earth data released by the Suzaku XIS team.

SAX J1748.2–2808 was also in the field of view of the XMM-Newton observations on Sgr D SNR and G 0.9+0.1 on September 2000 and March 2003, respectively. The pointing observation on SAX J1748.2–2808 was also made on February, 2005. The X-ray data were obtained with the European Photon Imaging Camera (EPIC) (Strüder et al. 2001; Turner et al. 2001) in an extended full-frame mode. The data were analyzed using the Science Analysis Software (SAS 7.1.0). Event files for both the PN and the Metal Oxide Semiconductor (MOS) detectors were produced using the `epchain` and `emchain` tasks of SAS, respectively. The event files were screened for high particle-background periods. Good exposure times are listed in table 1. In our analysis, we used the events corresponding to patterns 0–4 for the PN and 0–12 for the MOS instruments. The PN data of SAX J1748.2–2808 on the 2003 observation was not available.

### 3. Analysis and Results

#### 3.1. X-ray Image

The X-ray images taken with the XIS were analyzed for each observation separately. Since the Suzaku nominal position error is  $\lesssim 20''$  (Uchiyama et al. 2008), we fine-tuned the Suzaku position while referring to the positions of XMM-Newton sources. In the Sgr D SNR observation, we found an XMM-Newton source S10 (see table 4 of Sidoli et al. 2006). The XMM-Newton position of S10 is  $(\alpha, \delta) = (267^\circ 24531, -28^\circ 188918)$ , while the Suzaku position is  $(\alpha, \delta) = (267^\circ 24409, -28^\circ 185869)$ . We therefore shifted the Suzaku coordinate by  $(\Delta\alpha, \Delta\delta) = (0^\circ 00122, -0^\circ 003049)$ . In the G0.9+0.1 observation, we used an XMM source S2 (see table 4 of Sidoli et al. 2006). The XMM Newton position is  $(\alpha, \delta) = (266^\circ 81562, -28^\circ 181511)$ , while the Suzaku position is  $(\alpha, \delta) = (266^\circ 81737, -28^\circ 180065)$ . We hence shifted the Suzaku coordinate by  $(\Delta\alpha, \Delta\delta) = (-0^\circ 00175, -0^\circ 001446)$ . After these fine-tunings of the Suzaku coordinate, we made the X-ray image shown in figure 1. We found two sources near to the edge of each field. These two sources coincide in position with S3, i.e., SAX J1748.2–2808 (stronger source) and S12 (fainter source) of the XMM-Newton observation within statistical errors of  $\lesssim 5''$ .

In order to estimate the intensity ratio of the two sources, we made a projected profile along the line connecting SAX J1748.2–2808 and S12 (see figure 1c). The profile was fitted with two Gaussians plus a liner function, as is shown in figure 2. The widths ( $1-\sigma$ ) of the Gaussians approximate the projected point-spread function. The best-fit source fluxes (normalizations of the Gaussians) were determined to be  $7.5 \times 10^{-3}$  and  $2.8 \times 10^{-3}$  counts  $s^{-1}$ , for SAX J1748.2–2808 and for S12, respectively.

#### 3.2. Spectrum

Since the X-ray spectrum of XMM-Newton has already been reported, we show the Suzaku spectrum of SAX J1748.2–2808. The point-spread function of the XRT has a complicated polygon shape images, due together to the 4-segments structure of the XRT and image deformation near the field edge (Serlemitsos et al. 2007). We therefore extracted the spectra from the solid polygons in figures 1a and 1b, for the best S/N ratio within limited statistics.

The background spectra were obtained from a near-by sky shown by the dashed squares, from which the dashed elliptical regions were excluded. The background spectra consist of the non-X-ray background (NXB) and the local background (the cosmic X-ray background plus the Galactic center diffuse X-rays). Since the local background is affected by the vignetting of the XRT while the NXB is not, each background was treated separately. For both the source and the background data, we made COR distributions and composed the NXB spectra from the COR-sorted NXB data set (see section 2). We then subtracted the NXB extracted from the same detector areas. After NXB subtraction, we corrected the vignetting effect due to the different off-axis angles between the source and the background regions by multiplying the effective-area ratios for each energy bin of the local background spectra (the same process as Hyodo et al. 2008). We further subtracted the corrected local background from the source spectra. All of the source spectra of the two FIs from the two observations are co-added to increase the statistics.

We estimated the contamination of the near-by fainter source S12 by a ray-tracing simulation (`xissim` in the HEASoft package). The spectral shape of SAX J1748.2–2808 was assumed to be an absorbed power-law plus 3 Gaussian lines, whose parameters are the same as

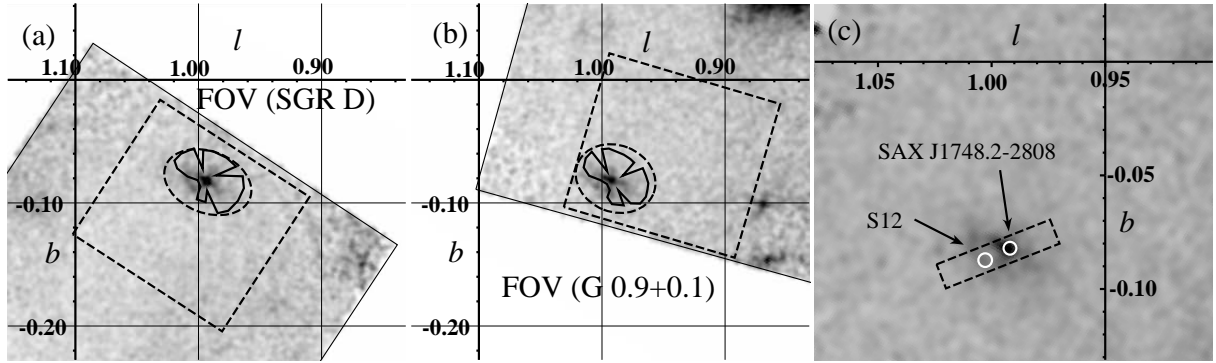


**Fig. 1.** X-ray image in the 3–7 keV band from the Suzaku observations on Sgr D SNR (a) and G 0.9+0.1 (b). The source regions of SAX J1748.2–2808 are given by the solid polygons, which trace the complicated point-spread function of the XRT in the field edge (see text). The dashed squares (excluding ellipses) are the local backgrounds. (c): Combined images of figures (a) and (b) near SAX J1748.2–2808. The projected profile (figure 2) was made from the dashed rectangle region, where the white circles indicate the positions of SAX J1748.2–2808 (stronger source) and S12 (fainter source) (Sidoli et al. 2006).

table 2. This spectral model will be mentioned in the next paragraph. Since the fainter source S12 is too weak to allow a spectral analysis, its spectral shape was assumed to be the same model of an absorbed black-body ( $N_{\text{H}} = 10^{24} \text{ cm}^{-2}$ ,  $kT = 1 \text{ keV}$ ) as Sidoli et al. (2006). Using the flux ratio of SAX J1748.2–2808 and S12 determined in section 3.1, we found that the contamination was  $\lesssim 10\%$  in the 3–10 keV band. We therefore ignore the contamination of S12 in the following analysis and discussion.

The X-ray spectra of FI and BI were simultaneously fitted with an absorbed power-law plus one broad line,  $\text{Abs} \times (\text{Power-Law} + 1 \text{ Gaussian line})$ , which is the same model as that of the XMM-Newton by Sidoli et al. (2006). The best-fit (90% confidence range) photon index of the power-law, line center energy, and width ( $1\sigma$ ) are 1.2 (0.8–1.5), 6.66 (6.54–6.77) keV, and 0.31 (0.21–0.39) keV, respectively ( $\chi^2/\text{dof}$  of 72.8/64). These parameter values are consistent with those of XMM-Newton within the statistical error. However, the Suzaku spectrum exhibits significant residuals near to energies of 6.4, 6.7, and 7.0 keV. We therefore fitted with a model of an absorbed power-law plus 3 narrow lines near to 6.40, 6.68 and 6.97 keV,  $\text{Abs} \times (\text{Power-Law} + 3 \text{ Gaussian lines})$ . Although the fittings were made simultaneously for the FI and BI spectra, we simply show the FI result in figure 3. The fit was improved with  $\chi^2/\text{dof}$  of 67.6/64. The best-fit parameters are listed in table 2.

The best-fit line energies of 6.7 keV and 7.0 keV are likely due to  $K\alpha$  lines from He-like and H-like irons at energies of 6.68 keV and 6.97 keV, respectively, while the 6.4 keV line would be a  $K\alpha$  line from neutral irons. The 6.97 keV line may be contaminated by a  $K\beta$  line (7.05 keV) of neutral irons. We therefore applied a more physical model: an absorbed thin thermal plasma (APEC) plus the 6.40 keV and 7.05 keV lines from neutral irons,  $\text{Abs} \times (\text{APEC} + 6.40 \text{ keV} + 7.05 \text{ keV lines})$ . In this model, we fixed the flux ratio of the 6.40 keV and 7.05 keV lines to 1:0.125 (Kaastra & Mewe 1993). A simultaneous fit for the FI and BI spectra with  $\chi^2/\text{dof}$  of 77.4/65 is acceptable at

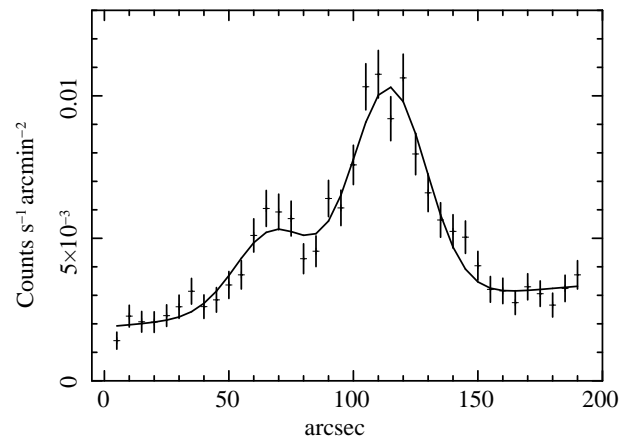


**Fig. 2.** Projected profile along the line connecting SAX J1748.2–2808 and S12. This profile was made from the data in the dashed rectangle in figure 1c. The solid lines are the best-fit liner function and 2-Gaussians.

the 90% confidence level, as is given in table 2. In figure 4, we show only the FI spectrum for simplicity.

### 3.3. Timing

We examined a long-term (8 years) X-ray flux history from the 5 observations listed in table 1. The X-ray fluxes were calculated by fitting the 3-line model with the parameters fixed values given in table 2. Only the normalization (flux) was a free parameter. The resultant fluxes in the 3–10 keV band show no significant variation during the 8 years interval.

We then searched for a coherent pulsation in the 3–7 keV band from all of the observations listed in table 1. The Fast Fourier Transform (FFT) analysis revealed a clear peak at  $\sim 1.7 \times 10^{-3} \text{ Hz}$  from all of the observations. We then searched for accurate pulse period with the folding technique, and found a significant peak near to the trial period of 593 sec. The best-fit pulse periods and errors are listed in table 3 for all of the observations. As an example, we show the Suzaku results from 2007: the

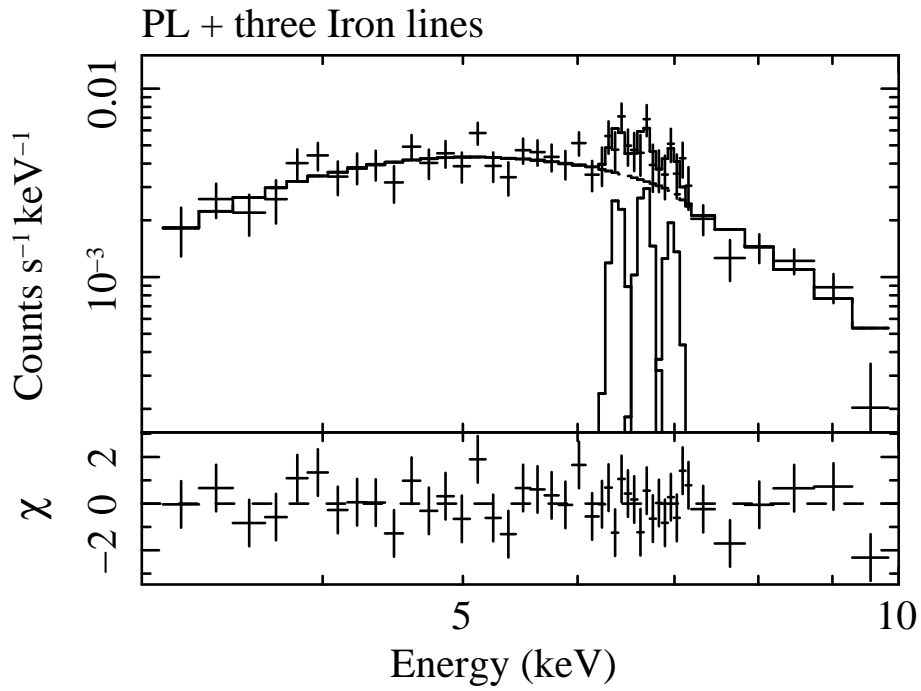


**Fig. 3.** Background-subtracted spectrum of SAX J1748.2–2808 for the FI CCD. The source spectrum was made from the solid polygons in figures 1a and 1b, while the local background spectra were taken from the dashed squares excluding the dashed ellipses. The solid line is the best-fit model of an absorbed power-law plus 3 Gaussians.

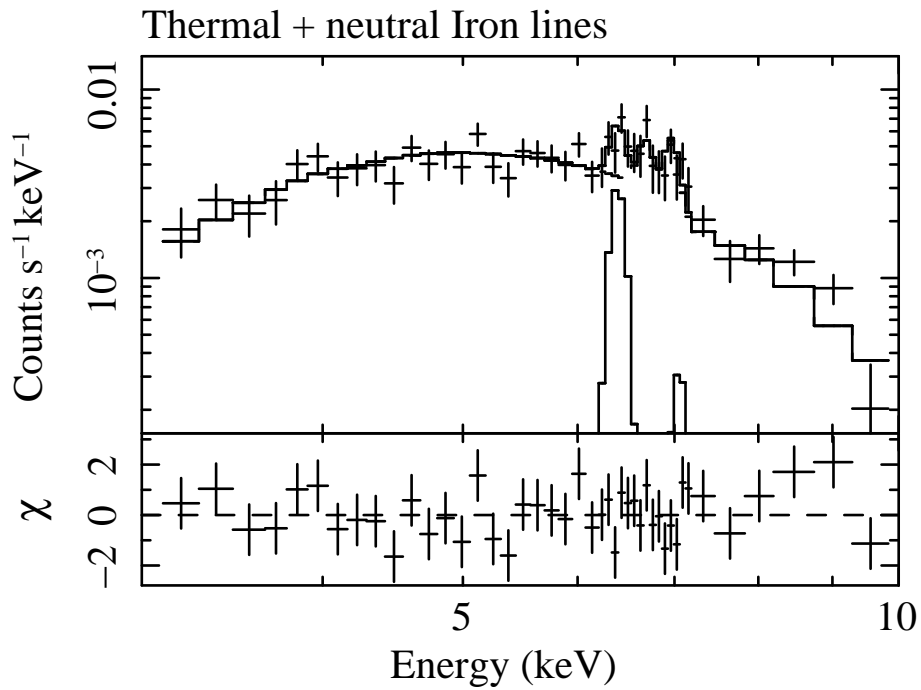


**Fig. 4.** Same as figure 3, but the best-fit model of an absorbed thin thermal plasma (APEC) plus K-shell lines of neutral iron.

**Table 2.** Best-fit parameters

Model: Abs×(Power-Law + 3 Gaussian Lines)		
Line Energy (keV)	Flux ( $10^{-6}$ ph s $^{-1}$ cm $^{-2}$ )	Equivalent Width (eV)
6.40 (6.39–6.47)	1.5 (0.8–2.3)	140 (30–270)
6.68 (6.66–6.72)	1.9 (1.1–2.7)	180 (30–350)
6.97 (6.94–7.46)	1.3 (0.6–2.1)	130 ( $\leq$ 270)
Parameter	Best-Fit Value	
Photon Index	1.0 (0.8–1.3)	
$N_{\text{H}}$ ( $10^{23}$ cm $^{-2}$ )	1.3 (1.0–1.7)	
Flux (3–10 keV) ( $10^{-13}$ erg s $^{-1}$ cm $^{-2}$ )	6.0 (5.7–6.2)	
Luminosity $^{\dagger}$ (3–10 keV) ( $10^{33}$ erg s $^{-1}$ )	7.4 (7.0–7.6)	
$\chi^2$ / dof	67.6 / 64	
Model: Abs×(APEC + Neutral Iron Lines)		
Line Energy (keV)	Flux ( $10^{-6}$ ph s $^{-1}$ cm $^{-2}$ )	Equivalent Width (eV)
6.40 (fixed)	2.1 (1.0–2.7)	160 (10–270)
7.05 (fixed)	0.26 $^{\ddagger}$	23
Parameter	Best-Fit Value	
Temperature: $kT$ (keV)	12 (9–17)	
Metal abundance (solar)	0.57 (0.35–0.85)	
$N_{\text{H}}$ ( $10^{23}$ cm $^{-2}$ )	1.8 (1.6–2.1)	
Flux (3–10 keV) ( $10^{-13}$ erg s $^{-1}$ cm $^{-2}$ )	5.4 (5.2–5.7)	
Luminosity $^{\dagger}$ (3–10 keV) ( $10^{33}$ erg s $^{-1}$ )	8.4 (8.0–8.8)	
$\chi^2$ / dof	77.4 / 65	

\* Parenthesis is 90% confidence range.

$^{\dagger}$  Absorption corrected. Distance toward SAX J1748.2–2808 is assumed to be 8.5 kpc.

$^{\ddagger}$  The flux of the 7.05 keV line is constrained to be 0.125 of the 6.40 keV Line.

power spectrum of FFT, periodogram, and folded light curve in figure 5a, 5b, and 5c, respectively.

The 593-sec pulsation is likely to be a spin rotation of either a magnetic white dwarf or a neutron star in a binary system (see section 4). We, therefore, searched for an orbital modulation in the light curve with 1000-sec binning. In the Suzaku observations, we found no sign of orbital modulation, nor any sign of an eclipse. And no orbital modulation was found from the XMM-Newton data, either. This is reasonable because the time coverages of the XMM-Newton observations were less than the Suzaku.

#### 4. Discussion

We found a coherent pulsation of 593-sec from SAX J1748.2–2808. This constrains the origin of this source to be either a magnetic CV, or a HMXB pulsar. The 593-sec period is among the slowest 10% of the pulse period in HMXB pulsars (Nagase et al. 1989, Liu et al. 2000), while the fastest 30% in magnetic CVs (Ritter & Kolb 2003). Thus, the spin period of 593-sec favors a magnetic CV scenario, although a HMXB pulsar scenario is not firmly excluded.

The Suzaku spectrum resolved the broad line at 6.6 keV found in the previous XMM-Newton observation into, at least, three lines at 6.40, 6.68, 6.97 keV. The best-fit equivalent width ( $EW$ ) of these three lines are  $\sim$ 140 eV,  $\sim$ 180 eV, and  $\sim$ 130 eV, respectively. Ezuka and Ishida (1999) compiled the ASCA data and reported that the

magnetic CVs exhibit 3 iron  $K\alpha$  lines at 6.4, 6.7, and 7.0 keV with mean  $EW$  values of  $\sim$ 100,  $\sim$ 200, and  $\sim$ 100 eV, respectively (see also Hellier et al. 1998), nearly the same as those of SAX J1748.2–2808.

The overall spectrum was also well fitted with a thin thermal plasma of 12-keV temperature with a sub-solar iron abundance plus  $K\alpha$  (6.40 keV) and  $K\beta$  (7.05 keV) lines from neutral irons. Ezuka and Ishida (1999) also reported that the spectra of the magnetic CVs can be described by a thin thermal plasma model plus 6.4 keV line with a mean temperature of  $\sim$ 20 keV, closely resemble to the Suzaku results of SAX J1748.2–2808. On the other hand, HMXB pulsars show a hard continuum spectrum, but it is a broken power-law and not a thin thermal. HMXBs exhibit an iron emission line feature. However, the line feature is not complex, but is a single line, mostly at 6.4 keV (see table 3 of Nagase et al. 1989). These properties are different from those of SAX J1748.2–2808.

All of the above facts favor the idea that SAX J1748.2–2808 is a magnetic CV rather than a HMXB. The pulse period of 593-sec is smaller than the possible orbital period, although we found no orbital modulation. Therefore, 593-sec would be the spin period, and hence SAX J1748.2–2808 is an intermediate polar (IP), not a polar with synchronized spin and an orbital period. If the luminosity of SAX J1748.2–2808 is typical value for an IP of  $\sim$   $10^{33}$  erg s $^{-1}$  (Patterson 1994), then from the observed flux of  $\sim$   $6 \times 10^{-13}$  erg cm $^{-2}$  s $^{-1}$ , the distance is estimated to be  $\sim$ 4 kpc. Thus, SAX J1748.2–2808 would

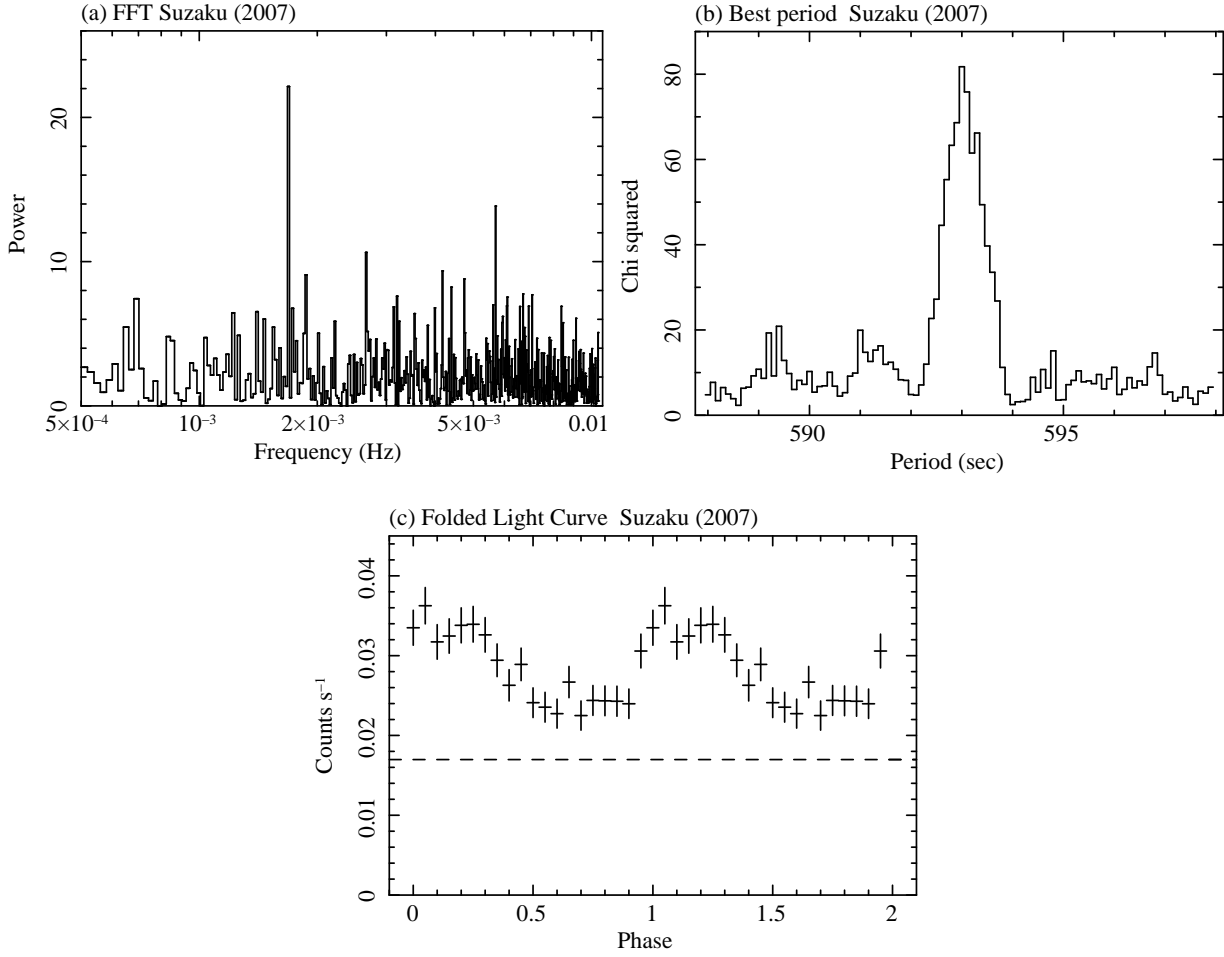


**Fig. 5.** (a): Power spectrum (FFT) in the 3–7 keV band of the Suzaku observation (2007). (b): Same as (a), but the periodogram at around the trial period of 593 sec. (c): Same as (a), but the folded light curve at the best-fit period of 593.1 sec, where the dashed line is the background level.

**Table 3.** Best-fit Period

Observatory (Year/Month)	Instruments	Pulse Period (s)
XMM-Newton (2000/09)	MOS1+2	$592 \pm 8$
XMM-Newton (2000/09)	PN	$594 \pm 8$
XMM-Newton (2003/03)	MOS1+2	$593 \pm 2$
XMM-Newton (2005/02)	MOS1+2	$595 \pm 3$
XMM-Newton (2005/02)	PN	$593 \pm 2$
Suzaku (2007/09)	XIS 0+1+3	$593.1 \pm 0.4$
Suzaku (2008/03)	XIS 0+1+3	$592.8 \pm 0.4$

\* Error is  $1\text{-}\sigma$  of the Gaussian of the folded result (e.g. figure 5b).

be a foreground source, not a member of the GC sources.

Conversely, Sidoli et al. (2006) suspected that SAX J1748.2–2808 is located near the GC region at about 8.5 kpc, because it has a large absorption of  $1.4 \times 10^{23} \text{ H cm}^{-2}$ . With this distance, they estimated the luminosity to be  $\sim 10^{34} \text{ erg s}^{-1}$ , significantly larger than any other magnetic CVs, and hence the authors declined to suggest a HMXB origin. We, however, note that a large fraction of the absorption of IPs is due to the circum-stellar gas, and the absorption value could be up to several  $\times 10^{23} \text{ H cm}^{-2}$  (Ezuka & Ishida 1999). Therefore, the large absorption of SAX J1748.2–2808 would also be due to circum-stellar gas, rather than interstellar gas integrated along the long line of sight. This large amount of circum-stellar gas can be naturally explained as being the origin of the strong 6.4 keV line from neutral irons (see e.g. Ezuka & Ishida 1999).

The authors thank all of the Suzaku team members, especially Y. Hyodo, H. Uchiyama, M. Ozawa, H. Nakajima, H. Yamaguchi, and H. Mori for their supports and useful information on the XIS performance. We also thank our referee, M. Ishida for his useful comments. This work is supported by Grant-in-Aids from the Ministry of Education, Culture, Sports, Science and Technology (MEXT) of Japan, Scientific Research A (KK), and Grant-in-Aid for Young Scientists B (HM). HM is also supported by the Sumitomo Foundation, Grant for Basic Science Research Projects, 071251, 2007. MN is supported by JSPS Research Fellowship for Young Scientists.

## References

- Ezuka, H. & Ishida, M. 1999, *ApJS*, 120, 277  
 Hellier, C., Mukai, K. & Osborne, J. P. 1998, *MNRAS*, 297, 526  
 Hyodo, Y., Tsujimoto, M., Hamaguchi, K., Koyama, K., Kitamoto, S., Maeda, Y., Tsuboi, Y., & Ezoe, Y. 2008, *PASJ*, 60, S85  
 Kaastra, J. S., & Mewe, R. 1993, *A&AS*, 97, 443  
 Koyama, K., et al. 2007a, *PASJ*, 59, S23  
 Koyama, K., et al. 2007b, *PASJ*, 59, S245  
 Liu, Q. Z., van Paradijs, J., & van den Heuvel, E. P. J. 2000, *A&AS*, 147, 25  
 Mitsuda, K., et al. 2007, *PASJ*, 59, S1  
 Munro, M. P., et al. 2003, *ApJ*, 589, 225  
 Munro, M. P., et al. 2004, *ApJ*, 613, 326  
 Munro, M. P., Bauer, F. E. Bandyopadhyay, R. M., & Wang, Q. D. 2006, *ApJS*, 165, 173  
 Nagase, F. 1989, *PASJ*, 41, 1  
 Patterson, J. 1994, *PASP*, 106, 209  
 Ritter, H. & Kolb, U. 2003, *A&A*, 404, 301  
 Serlemitsos, P., et al. 2007, *PASJ*, 59, S9  
 Sidoli, L., Mereghetti, S., Treves, A., Parmar, A. N., Turolla, R., & Favata, F. 2001, *A&A*, 372, 651  
 Sidoli, L., Mereghetti, S., Favata, F., Oosterbroek, T., & Parmar, A. N. 2006, *A&A*, 456, 287  
 Strüder, L., et al. 2001, *A&A*, 365, L18  
 Tawa, N., et al. 2008, *PASJ*, 60, S11  
 Turner, M. J. L., et al. 2001, *A&A*, 365, L27  
 Uchiyama, H., et al. in prep.

Uchiyama, Y., et al. 2008, *PASJ*, 60, S35